Proc. NIPR Symp. Polar Meteorol. Glaciol., **1**, 113–121, 1987

EVAPORATION FORM OF ICE CRYSTALS IN SUBSATURATED AIR AND THEIR EVAPORATION MECHANISM

Takehiko GONDA and Tadanori SEI

Faculty of Science and Technology, Science University of Tokyo, 2641, Higashi-Kameyama, Yamazaki, Noda 287

Abstract: The evaporation form and the evaporation mechanism of dendritic ice crystals grown in air of 1.0×10^5 Pa and at water saturation and polyhedral ice crystals grown in air of 4.0×10 Pa and at relatively low supersaturation are studied. In the case of dendritic ice crystals, the evaporation preferentially occurs in the convex parts of the crystal surfaces and in minute secondary branches. On the other hand, in the case of polyhedral ice crystals, the evaporation preferentially occurs in the parts where screw dislocations or stacking faults emerge. On the basis of these experimental results, the formation mechanism of single bullets observed at Mizuho Station, Antarctica is inferred.

1. Introduction

The growth form and the growth mechanism of ice crystals have been studied by many authors (KOBAYASHI, 1961; GONDA, 1980; BECKMANN and LACMANN, 1982; KURODA and LACMANN, 1982; YAMASHITA and ASANO, 1984; GONDA and SEI, 1987, etc.), but the evaporation form and the evaporation mechanism of ice crystals have not ever been studied. On the other hand, snow crystals formed in natural clouds are probable to evaporate below the cloud base because below the cloud base, snow crystals are exposed under the condition of ice subsaturation. Accordingly, it is important to study not only the growth form but also the evaporation form of ice crystals in order to presume the formation condition of snow crystals observed on the earth. In addition, it is important to study the evaporation form as well as the growth form of ice crystals for understanding the formation mechanism of snow crystals observed in Antarctica where many of snow crystals may be precipitated at a humidity just above and just below ice saturation.

KIKUCHI (1968) inferred that a single bullet was formed by the separation of a combination of bullets during a free fall. Thereafter, single bullets were also observed by the other authors (SHIMIZU, 1963; KIKUCHI and YANAI, 1971; WADA and GONDA, 1985; IWAI, 1986).

The purpose of this paper is to study the evaporation form and the evaporation mechanism of dendritic ice crystals grown in air of 1.0×10^5 Pa and at water saturation and polyhedral ice crystals grown in air of 4.0×10 Pa and at relatively low supersaturation, and to presume experimentally the formation mechanism of single bullets observed at Mizuho Station, Antarctica (WADA and GONDA, 1985) in order to clarify KIKUCHI's hypothesis (1968), too.

2. Experimental

A cold chamber used for the growth and evaporation experiments of dendritic ice crystals growing in air of 1.0×10^5 Pa and at water saturation is described in a previous paper (GONDA and YAMAZAKI, 1982). Minute ice crystals were formed in air of 1.0×10^5 Pa and at $-15°C$, by supplying silver iodide smoke into the cold chamber. Only one of ice crystals nucleated in air was received on a cover glass previously cooled down to a desired temperature, and the ice crystal was grown at $-15°C$ and water saturation. The dendritic ice crystal grown under the condition described here was evaporated at a subsaturation near ice saturation, and the evaporation form was observed using a differencial interference microscope.

Next, a cold chamber used for the growth and evaporation experiments of polyhedral ice crystals in air of 4.0×10 Pa is described in a previous paper (GONDA and KOIKE, 1982). Polyhedral ice crystals were grown in air of 4.0×10 Pa at -7, -15 and $-30°C$ and relatively low supersaturation and then were evaporated at relatively low subsaturation. The evaporation form was observed using the same microscope as that described above.

The reason why the evaporation experiments of ice crystals were carried out in air of 1.0×10^5 and 4.0×10 Pa is to check the effects of the existence of air on the evaporation form and the evaporation mechanism of the ice crystals.

3. Experimental Results

3.1. Evaporation form of dendritic ice crystals in air of 1.0×10^5 Pa and at a subsaturation near ice saturation

Figure 1 shows a dendritic ice crystal with minute secondary branches growing in air of 1.0×10^5 Pa and at $-15°C$ and water saturation (a–d) and then evaporating at a subsaturation near ice saturation at $-15°C$ (e–h). As shown in the figure, in the evaporation stage, as the convex parts on the {0001} face and minute secondary branches

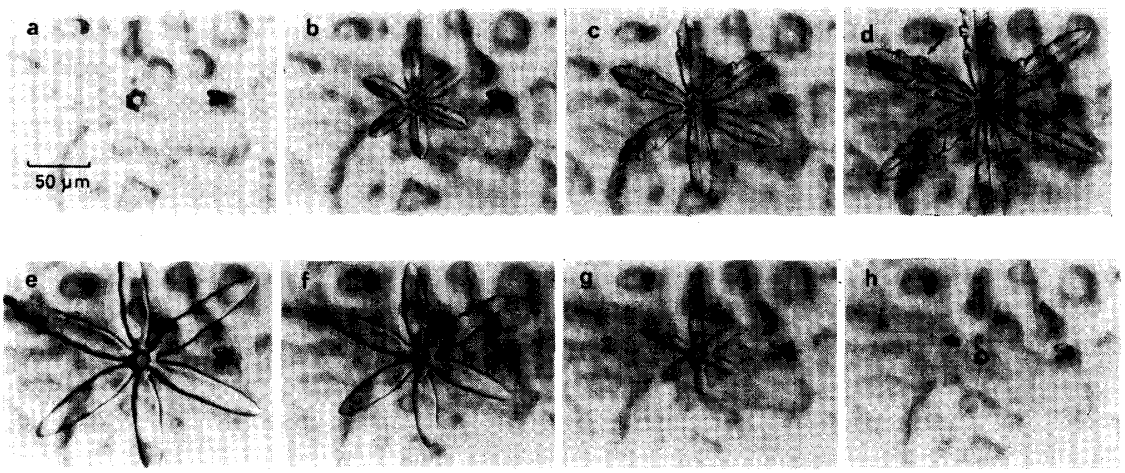

Fig. 1. Dendritic ice crystal growing in air of 1.0×10^5 Pa and at $-15°C$ and water saturation (a–d) and then evaporating at a subsaturation near ice saturation (e–h). (a) 0, (b) 50, (c) 95, (d) 140 s; (e) 0, (f) 30, (g) 60, (h) 70 s.

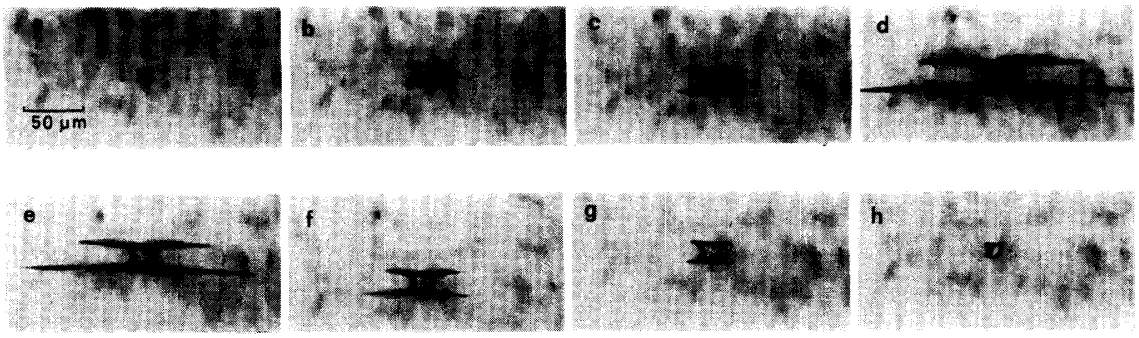

Fig. 2. Dendritic ice crystal growing in air of 1.0×10^5 Pa and at -15°C and water saturation (a–d) and then evaporating at a subsaturation near ice saturation (e–h). (a) 0, (b) 35, (c) 60, (d) 190 s; (e) 0, (f) 15, (g) 25, (h) 35 s.

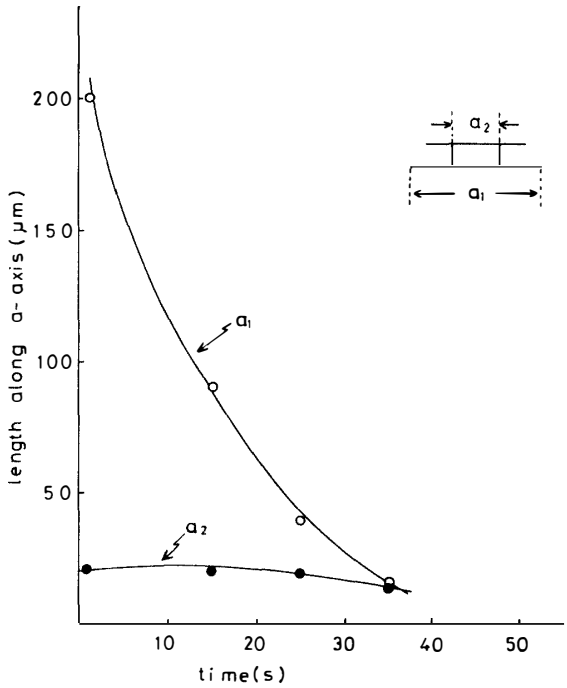

Fig. 3. Length along a-axis of a dendritic ice crystal grown in air of 1.0×10^5 Pa and -15°C and water saturation vs. time elapsed when the ice crystal evaporates.

(arrow ↑) preferentially evaporate, the ice crystal surface becomes smooth. After that, the top of primary branches evaporates with the lapse of time (f and g).

Figure 2 shows a dendritic ice crystal growing in air of 1.0×10^5 Pa and at -15°C and water saturation (a–d) and then evaporating at a subsaturation near ice saturation at -15°C (e–h), which was photographed from the direction along the b-axis. In the growth stage, it is seen that there are the convex parts on both the {0001} and $\{10\bar{1}0\}$ faces and under the condition of -15°C and water saturation, the crystal with dendritic plates on the top and the bottom of the columnar part finally grows. After that this crystal was evaporated at a subsaturation near ice saturation (e–h). As shown in the figure, the minute convex parts on the $\{10\bar{1}0\}$ face as well as those on the {0001} face preferentially evaporate, and as a result, the ice crystal surface became

smooth (e). In the next stage, the top of the primary branches evaporates with the lapse of time (f and g).

Figure 3 shows an example of the length along *a*-axis of a dendritic ice crystal grown in air of 1.0×10^5 Pa and at $-15°C$ and water saturation versus time elapsed when the ice crystal evaporates. In the evaporation stage, the columnar part (a) with dendritic plates on the top and the bottom is almost constant with the time elapsed. On the contrary, it is seen that the parts which correspond to the primary branches (a) abruptly decrease with the lapse of time.

3.2. *Surface structure of polyhedral ice crystals evaporating in air of 4.0×10 Pa and at relatively low subsaturation*

Dendritic ice crystals are formed when ice crystals grow in air of 1.0×10^5 Pa and at water saturation, under which the resistance of volume diffusion process of water molecules is very large. On the contrary, polyhedral ice crystals are formed when ice crystals grow in air of low pressure and at relatively low supersaturation, under which the resistance of volume diffusion of water molecules can be ignored.

Figure 4 shows the surface structure of the {0001} face of a polyhedral ice crystal growing in air of 4.0×10 Pa at $-30°C$ and 1.8% supersaturation (a and b) and then evaporating at 0.6% subsaturation at $-30°C$ (c–f). In Fig. 4 (b and d), the bold lines running obliquely from the top of the left to the bottom of the right are the video scanning lines. In the growth stage (a and b), it is seen that the growth steps move from the centers of screw dislocations (arrow ↑) emerging near the corner of the crystal to a center of the crystal. On the contrary, in the evaporation stage (c–f), it is seen that the evaporation steps advance from the centers of screw dislocations emerging

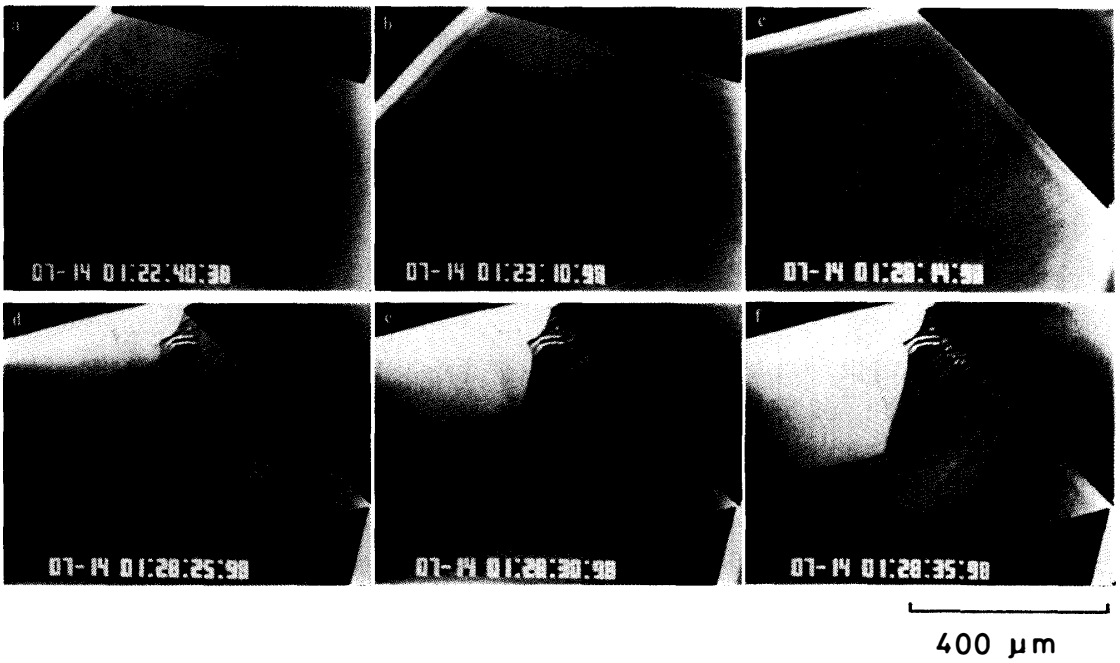

Fig. 4. Surface structure of the {0001} face of a polyhedral ice crystal growing in air of 1.0×10 Pa at $-30°C$ and 1.8% supersaturation (a, b) and then evaporating at 0.6% subsaturation (c–f). (a) 0, (b) 30 s; (c), 0, (d) 11, (e) 16, (f) 21 s.

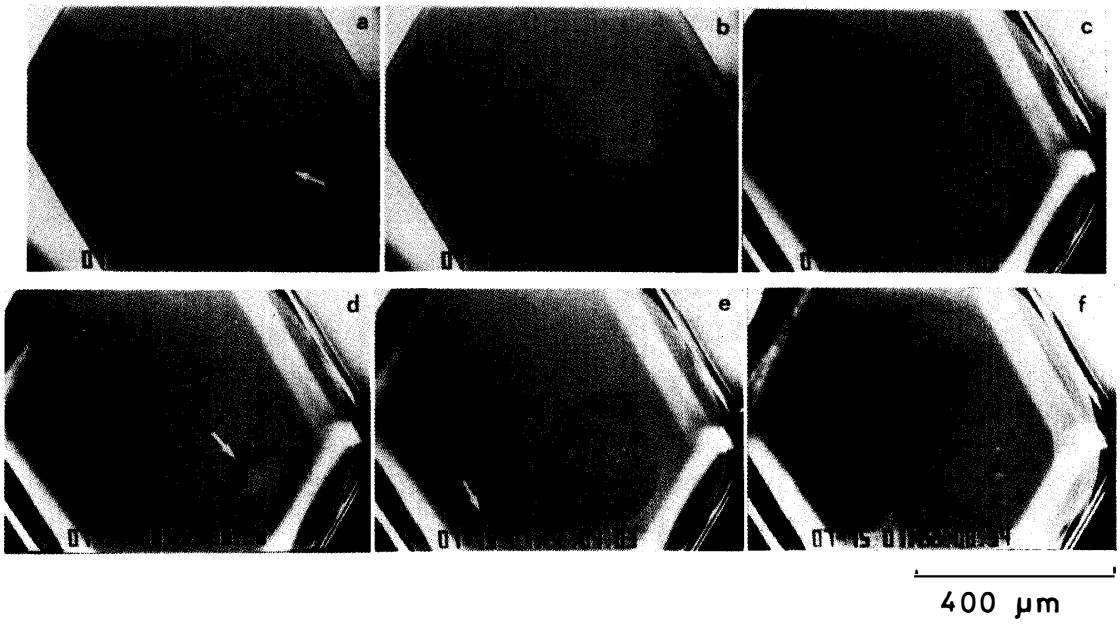

Fig. 5. Surface structure of the {0001} face of a polyhedral ice crystal growing in air 1.0 × 10 Pa at −7°C and 2.0% supersaturation (a, b) and then evaporating at 6.0% subsaturation (c–f). (a) 0, (b) 2 s; (c) 0, (d) 0.5, (e) 1.0, (f) 4.5 s.

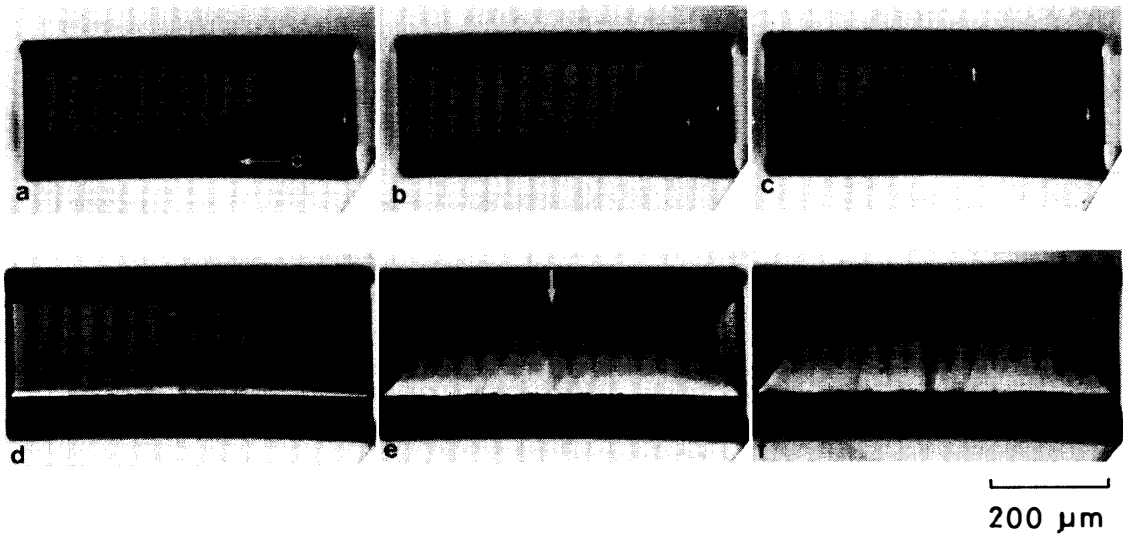

Fig. 6. Surface structure of the {10$\bar{1}$0} face of a polyhedral ice crystal growing in air of 4.0 × 10 Pa at −15°C and 2.0 supersaturation (a–c) and then evaporating at a subsaturation near ice saturation (d–f). (a) 0, (b) 9, (c) 19 s; (d) 0, (e) 27, (f) 54 s.

near the corner of the crystal to a center of the crystal (c). In the next stage, the evaporation takes place as if we cut the {0001} face at an angle because the evaporation preferentially occurs at the edges of the crystal with the lapse of time. It is considered that the streaks running from the crystal edges to a center of the crystal were formed by the impurities adsorbed on the crystal surface in the growth process.

Figure 5 shows the surface structure of the {0001} face of a polyhedral ice crystal growing in air of 4.0 × 10 Pa at −7°C and 2.0% supersaturation (a and b) and then

evaporating at 6.0% subsaturation at $-7°C$ (c–f). In Fig. 5 (a and b), the bold lines running obliquely from the top of the left to the bottom of the right are the video scanning lines. It can be understood from the growth hillock emerging on the {0001} face that the source of growth steps is the screw dislocation emerging on the {0001} face. In the case of evaporation stage (c–f), it is understood from the evaporation pits emerging on the {0001} face that the source of the evaporation steps is the screw dislocation emerging on the {0001} face. That is to say, when screw dislocations emerge on the crystal surface, the growth steps or the evaporation steps advance from the center of screw dislocations under low supersaturation or under low subsaturation, respectively.

Figure 6 shows the surface structure of the $\{10\bar{1}0\}$ face of a polyhedral ice crystal growing in air of 4.0×10 Pa at $-15°C$ and 2.0% supersaturation (a–c) and then evaporating at a subsaturation near ice saturation at $-15°C$ (d–f). In the growth stage (a–c), the boundary lines formed by the collision of growth steps which come from the opposite side are seen. In the evaporation stage (d–f), the evaporation preferentially occurs at the position where a stacking fault proposed by KOBAYASHI and OHTAKE (1974) emerges perpendicularly to the c-axis near the center of the $\{10\bar{1}0\}$ face in addition to the evaporation at the edges of the $\{10\bar{1}0\}$ face; at 27 min after the evaporation, the linear concave is observed near the center of the $\{10\bar{1}0\}$ face (arrow ↑ in photo e). At 54 min after the evaporation (f), the ridges characteristic of the evaporation are seen as a result of the disappearance of the $\{10\bar{1}0\}$ face.

Figure 7 shows the surface structure of the $\{10\bar{1}0\}$ face of polyhedral ice crystal evaporating in air of 4.0×10 Pa at $-7°C$ and a subsaturation near ice saturation

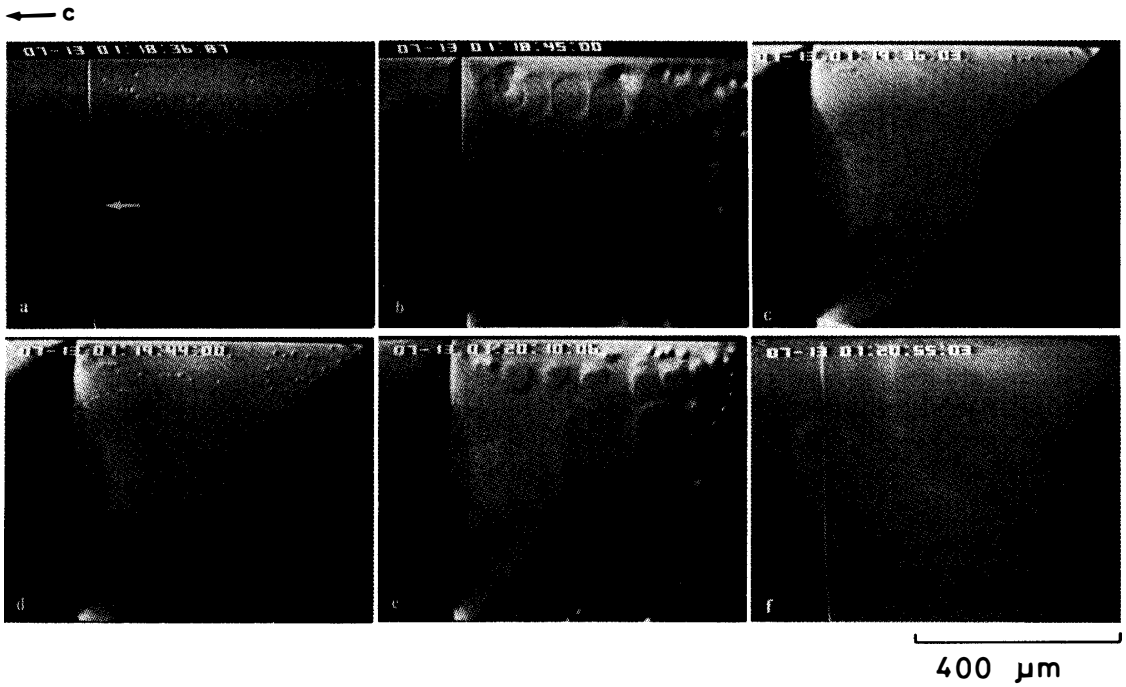

Fig. 7. Surface structure of the $\{10\bar{1}0\}$ face of a polyhedral ice crystal evaporating in air of 4.0×10 Pa at $-7°C$ and a subsaturation near ice saturation (a, b) and then growing at a supersaturation near ice saturation (c–f). (a) 0, (b) 9 s; (c) 0, (d) 8, (e) 34, (f) 74 s.

(a and b) and then growing at a supersaturation near ice saturation at $-7°C$ (c–f). In the evaporation stage, the evaporation preferentially occurs at the portions where a stacking fault running perpendicularly to the *c*-axis near the center of the $\{10\bar{1}0\}$ face and screw dislocations emerge. As a result, a linear concave formed by evaporation (arrow ↑) and many evaporation pits are seen. At 9 s after the evaporation (b), the advance of evaporation steps is seen. In the earlier growth stage (c), many growth hillocks are formed together with the traces of the ridges formed during the evaporation process. At 8 s after the transformation into the growth stage (d), the $\{10\bar{1}0\}$ face was formed on the ridges, and at the same time, the growth hillocks began to grow. At 34 s after the growth (e), the $\{10\bar{1}0\}$ face began to form by the sweeping of the growth steps. At 74 s after the growth (f), the $\{10\bar{1}0\}$ face is formed and it is seen that the growth steps come from the active screw dislocation emerging at the corner of the top of the right.

4. Discussion

It was found that the minute convex parts on the $\{0001\}$ and $\{10\bar{1}0\}$ faces and minute secondary branches of dendritic ice crystals grown in air of 1.0×10^5 Pa preferentially evaporated and then the top of the primary branches evaporated. This experimental fact can be explained by the reason described below. That is to say, the saturation vapor pressure over minute convex parts of the $\{0001\}$ and $\{10\bar{1}0\}$ faces and minute secondary branches is higher than that over plane surfaces in accordance with the curvature effect of the surface tension (Gibbs-Thomson's effect). Accordingly, the minute convex parts and the minute secondary branches of the dendritic ice crystal evaporate when the vapor pressure holds at a subsaturation near ice saturation.

In the next place, it was found that the evaporation of a polyhedral ice crystal grown in air of 4.0×10 Pa preferentially occurs in the portions where the screw dislocation and the stacking fault emerge. This is because the chemical potential of the portions where the screw dislocation and the stacking fault emerge is higher than that of the other portion. The reason why the evaporation experiments of ice crystals were carried out in air of 1.0×10^5 and 4.0×10 Pa is to check the effects of the existance

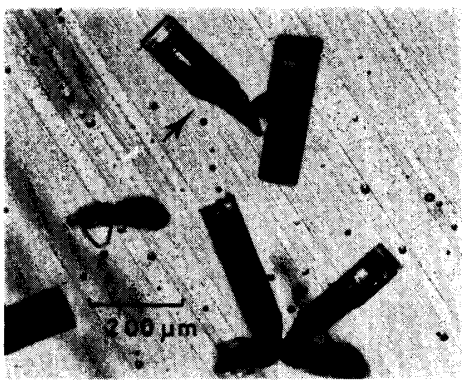

Fig. 8. Snow crystals observed at Mizuho Station, Antarctica on March 20, 1979 (WADA and GONDA, 1985).

of air on the evaporation form and the evaporation mechanism of the ice crystals.

Figure 8 shows an example of snow crystals observed at Mizuho Station, Antarctica on March 20, 1979 (WADA and GONDA, 1985). As shown in the figure, though the corners and edges of a single bullet are very sharp, the external form of its narrow part is considerably irregular. The former means that the single bullet was not formed by the evaporation of the combination of bullets because if the single bullet was exposed under a subsaturation over ice, whether its external form is deformed or its corners and edges evaporate and must be cut at an angle. On the other hand, the latter means that the single bullet was not exposed under a supersaturation over ice after the formation of the single bullet because if the single bullet was exposed under a supersaturation over ice, its irregular part grows and must become sharp. Accordingly, it is inferred that the single bullet observed at Mizuho Station was formed under ice saturation by the breaking of the combination of bullets due to the external force during a free fall.

5. Conclusions

The evaporation form and the evaporation mechanism of dendritic ice crystals growing in air of 1.0×10^5 Pa and polyhedral ice crystals growing in air of 4.0×10 Pa were studied. According to the experimental results, the formation mechanism of single bullets observed at Mizuho Station, Antarctica was inferred. The results obtained in this study are as follows.

1) The evaporation of dendritic ice crystals grown in air of 1.0×10^5 Pa preferentially occurs in the convex portions of the $\{0001\}$ and $\{10\bar{1}0\}$ faces and in the minute secondary branches, and then the top of primary branches evaporates.

2) The evaporation of polyhedral ice crystals grown in air of 4.0×10 Pa preferentially occurs in the portions where screw dislocations and stacking faults emerge, and then the corners and edges of the crystals evaporate.

3) It is inferred that the single bullets observed at Mizuho Station, Antarctica are formed not only by the evaporation of the combination of bullets but also by the breaking of the combination of bullets due to the external force during a free fall.

References

BECKMANN, W. and LACMANN, R. (1982): Interface kinetics of the growth and evaporation of ice single crystals from the vapor phase. Measurements in a pure water vapour environment. J. Cryst. Growth, **58**, 433–442.

GONDA, T. (1980): The influence of the diffusion of vapor and heat on the morphology of ice crystals grown from the vapor. J. Cryst. Growth, **49**, 173–181.

GONDA, T. and KOIKE, T. (1982): Growth rates and growth forms of ice crystals grown from the vapor phase. J. Cryst. Growth, **56**, 259–264.

GONDA, T. and SEI, T. (1987): The growth mechanism of ice crystals grown in air at a low pressure and their habit change with temperature. J. Phys., **48**, 355–359.

GONDA, T. and YAMAZAKI, T. (1982): Morphological stability of polyhedral ice crystals grown from the vapor phase. J. Cryst. Growth, **60**, 259–263.

IWAI, K. (1986): Morphological features of combination of bullet-type snow crystals observed at Syowa Station, Antarctica. Mem. Natl Inst. Polar Res., Spec. Issue, **45**, 38–46.

KIKUCHI, K, (1968): On snow crystals of bullet type. J. Meteorol. Soc. Jpn., **46**, 128–132.

KIKUCHI, K. and YANAI, K. (1971): Observation on the shapes of snow crystals in the South Pole region in the summer. Nankyoku Shiryô (Antarct. Rec.), **41**, 34–41.

KOBAYASHI, T. (1961): The growth of snow crystals at low supersaturations. Philos. Mag., Ser. 8, **6**, 1363–1370.

KOBAYASHI, T. and OHTAKE, T. (1974): Hexagonal twin prisms of ice. J. Atmos. Sci., **31**, 1377–1383.

KURODA, T. and LACMANN, R. (1982): Growth kinetics of ice from vapour phase and its growth forms. J. Cryst. Growth, **56**, 189–205.

SHIMIZU, H. (1963): "Long prism" crystal observed in the precipitation in Antarctica. J. Meteorol. Soc. Jpn., **41**, 305–307.

WADA, M. and GONDA, T. (1985): Snow crystals of hollow-prism type observed at Mizuho Station, Antarctica. Nankyoku Shiryô (Antarct. Rec.), **86**, 1–8.

YAMASHITA, A. and ASANO, A. (1984): Morphology of ice crystals grown from the vapour at temperatures between −4 and −1.5°C. J. Meteorol. Soc. Jpn., **62**, 140–145.

(Received April 30, 1987; Revised manuscript received May 30, 1987)